Supernova Remnants: An Odyssey in Space after Stellar Death III
9-15 June, 2024, Chania, Crete, Greece

Molecular formation in the ejecta of SN 1987A based on three-dimensional hydrodynamical models

Masaomi Ono (ASIAA), Takaya Nozawa (NAOJ), Shigehiro Nagataki (RIKEN), Alexandra Kozyreva (HITS), Salvatore Orlando (INAF), Marco Miceli (Univ. of Palermo), and Ke-Jung Chen (ASIAA)

Abstract

Motivated by the three-dimensional (3D) molecular distribution in supernova ejecta observed by ALMA, we solve time-dependent rate equations for chemical reactions, for the first time, based on 3D hydrodynamical simulations of core-collapse supernova (CCSN) explosions. In particular, the impact of matter mixing, affected by a bipolar-like explosion, on the formation of molecules is investigated. The energy deposition by the decay of radioactive ^{56}Ni (practically ^{56}Co) and consequent Compton electrons heat the gas, ionize species, and destroy molecules. The characteristic distribution of ^{56}Ni reflected by the matter mixing could non-negligibly affect the formation and destruction of molecules. See, ***MO et al. 2024, ApJS, 271, 33***, for the details.

Introduction

SN 1987A has provided many observational clues to understand the evolution of a CCSN thanks to its proximity and youth. SN 1987A is a unique object for elucidating the early evolution toward a supernova remnant. Early observations of SN 1987A such as iron lines (Haas et al. 1990) have indicated matter mixing in the supernova ejecta. We previously performed (MO et al. 2020) 3D hydrodynamical simulations for SN 1987A to address the mixing mechanism; an asymmetric bipolar-like explosion of a binary merger progenitor (Urushibata et al. 2018) reproduces the iron lines. A further evolution with additional 3D magnetohydrodynamics (Orlando et al. 2020) also explains the observed SN 1987A X-ray light curves.

Recent breakthrough observations of SN 1987A by ALMA (Abellán et al. 2017, see **Figure 1**) have revealed 3D distributions of carbon monoxide (CO) and silicon monoxide (SiO) in the ejecta. Those are rather clumpy and aspherical; CO seems to have a ring-like structure. ***To investigate the impact of matter mixing on molecular formation***, rate equations of chemical reactions are solved (MO et al. 2024) based on the 3D hydrodynamical models of SN 1987A (MO et al. 2020).

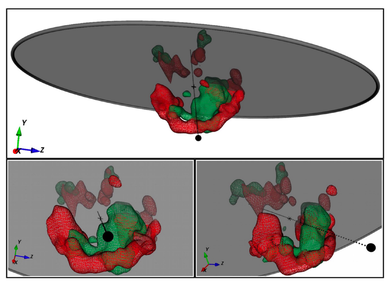

Figure 1 3D Distribution of CO (red) and SiO (green) in the ejecta of SN 1987A observed by ALMA (***Abellán et al. 2017***). The grey plane: the Equatorial Ring in the nebula. The dotted line with a black point: observer direction.

Method and Initial conditions

Initial condition: One-dimensional (1D) radial profiles of variables derived based on the 3D model for SN 1987A (MO et al. 2020, see **Figure 2**). Angle-averaged; angle-specified (the stronger and weaker bipolar explosion axes, and perpendicular to those, i.e., *+Z*, *−Z*, and *+Y* axes, respectively) 1D profiles are derived. ***1D hydrodynamical simulation***: 1D hydrodynamical simulations with the same hydrodynamical code as the 3D model (FLASH; Fryxell et al. 2000) are performed for up to 10,000 days. ***Tracer particles***: 100 tracer particles are radially distributed for obtaining Lagrangian time evolution. Then, the time evolution of the physical quantities of each particle is derived from the 1D simulation results.

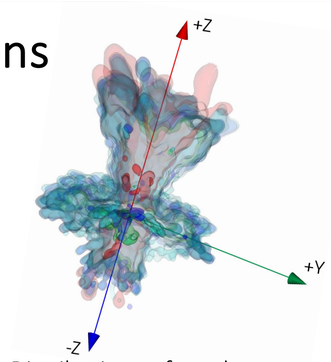

Figure 2 Distributions of seed atoms, iron (red), silicon (green), oxygen (blue), and carbon (cyan), in the ejecta of SN 1987A (MO et al. 2020). *+Z* (*−Z*) axis is directed to the stronger (weaker) bipolar-like explosion axis. *+Y* axis is perpendicular to the former.

Chemical reaction calculations: a chemical reaction network including 75 species: 24 diatomic molecules (H_2, CH, C_2, CN, CO, CS, NH, N_2, NO, OH, O_2, MgO, MgS, SiH, SiC, SiN, SiO, Si_2, SiS, SO, S_2, FeO, FeS, and Fe_2); 11 atoms; electrons; 39 singly-ionized ions is constructed. The reaction rates are adopted from the UMIST database (McElroy et al. 2013) and supplemented by others (e.g., Cherchneff & Dwek 2009; Sluder et al. 2018). Thermal fragmentation reactions and ionization/dissociation of species by Compton electrons produced via the decay of ^{56}Ni ($\rightarrow$ ^{56}Co $\rightarrow$ ^{56}Fe) are included. The time evolution of thermal quantities is re-calculated to include the *heating of the gas by the energy deposition via the decay of ^{56}Ni* and *cooling by rovibrational transitions of CO*. The rate equations for CO vibrational transitions are solved considering excitation/de-excitation of vibrational levels by electron collision and interaction with the background radiation. The electron impact excitation/de-excitation rates, rovibrational energy levels, statistical weights, and Einstein coefficients are adopted from the Refs. (Popalić et al. 2008; Li et al. 2015). The background radiation relies on a 1D radiation hydrodynamical simulation with the same initial condition (Kozyreva et al., in prep.). For each particle, the rate equations for chemical reactions are solved with the time evolution of the gas density and temperature as post-processing.

Initial distributions of seed atoms and ^{56}Ni

The initial distributions of seed atoms in the 1D profiles derived from the 3D model (MO et al. 2020) are shown (**Figures 3 and 4**). The characteristic distribution of ^{56}Ni plays a role in the formation and destruction of molecules as shown later.

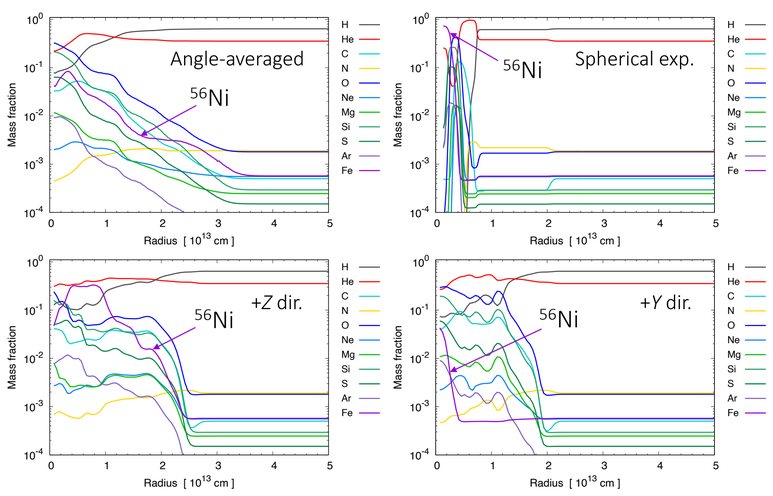

Figure 3 Initial distributions of seed atoms. Iron (Fe: purple) in inner metal-rich ejecta corresponds to ^{56}Ni. ***Left***: angle-averaged 1D profiles. ***Right***: the case of the purely spherical explosion.

Figure 4 Same as Figure 3 but for the following. ***Left***: 1D profiles in the *+Z* direction of the 3D model. ***Right***: ones in the *+Y* direction.

Results

i) Spherical vs Effective matter mixing by Angle-averaging of the 3D model

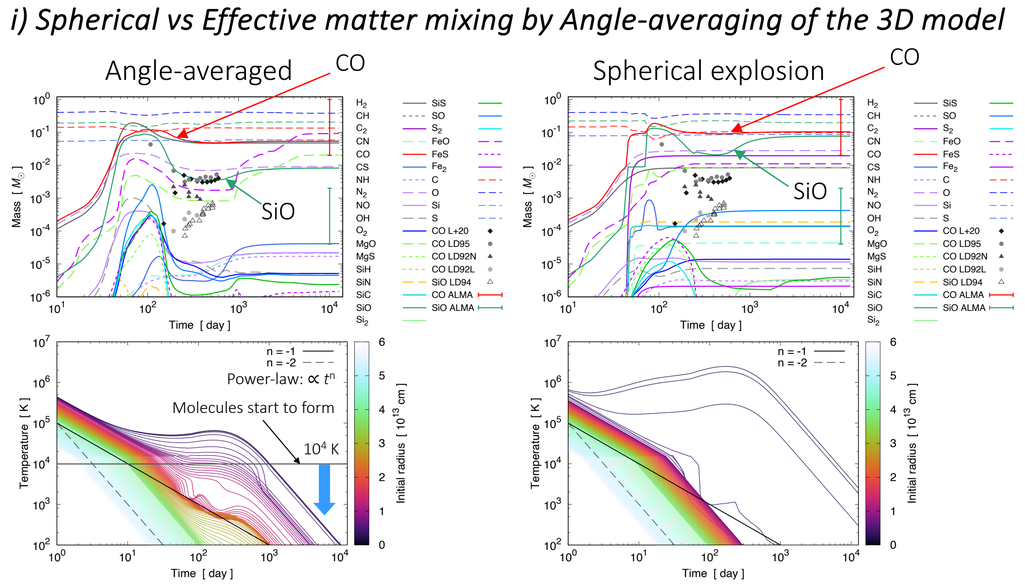

Figure 5 ***Top***: time evolution of the total masses of molecules and some of the seed atoms; points and vertical bars with errors are estimations by previous studies. ***Bottom***: time evolution of the gas temperatures of the tracer particles; colors denote the particles' initial positions (radii). ***Left***: results with angle-averaged 1D profiles (with effective matter mixing). ***Right***: the case of the purely spherical explosion.

ii) Contributing reactions for CO/SiO formation and destruction

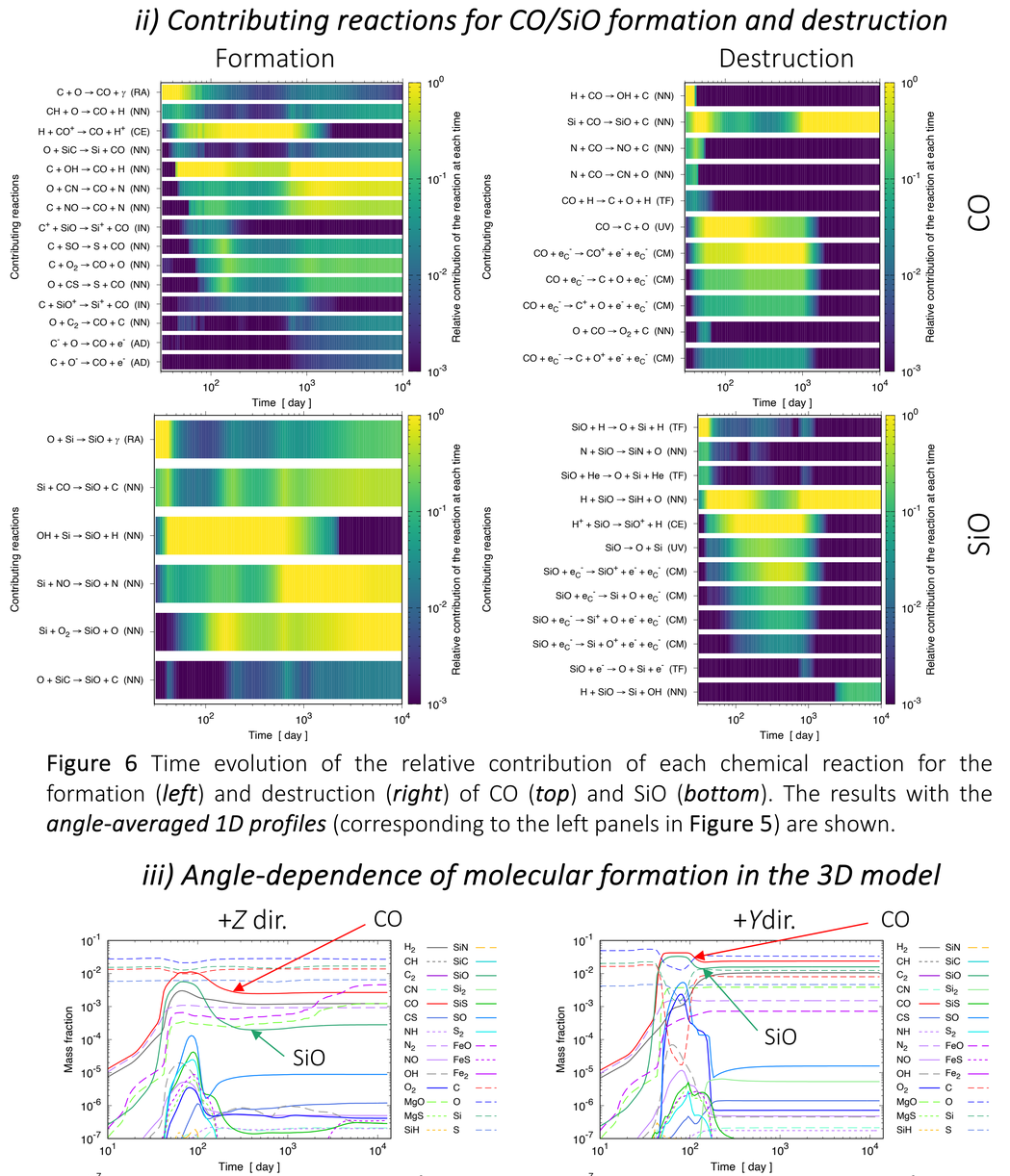

The code in the parentheses after each reaction denotes the rection type: **RA** (radiative association); **CE** (charge exchange); **IN** (ion-neutral); **AD** (associative electron detachment); **NN** (neutral-neutral); **CM** (Compton electron-induced); **UV** (dissociation by UV photons) **TF** (thermal fragmentation);

Figure 6 Time evolution of the relative contribution of each chemical reaction for the formation (***left***) and destruction (***right***) of CO (***top***) and SiO (***bottom***). The results with the ***angle-averaged 1D profiles*** (corresponding to the left panels in **Figure 5**) are shown.

iii) Angle-dependence of molecular formation in the 3D model

Figure 7 ***Top***: time evolution of the total mass fractions (not masses) of molecules and some of the seed atoms. ***Bottom***: Same as Figure 5. ***Left***: results along *+Z* direction. ***Right***: ones along *+Y* direction.

Summary

The asymmetric bipolar-like explosion and consequent matter mixing in the 3D model result in characteristic distributions of the seed atoms and the radioactive ^{56}Ni before molecules start to form. The energy deposition from the decay of ^{56}Ni causes the heating of the gas, ionization of species, and dissociation of newly formed molecules. The heating by the decay retards the formation of molecules, and ionization and dissociations could non-negligibly affect the destruction of molecules through Compton electron-induced (CM*), charge exchange (CE*), and ion-neutral (IN*) reactions. [* See, the legends in **Figure 6** for corresponding reactions]

Acknowledgment

MO acknowledges the support from the Pioneering Program of RIKEN for Evolution of Matter in the Universe (r-EMU) and RIKEN Interdisciplinary Theoretical and Mathematical Sciences Program (iTHEMS). This work is supported by JSPS KAKENHI Grant Number 19H00693 and JP21K03545. MO and KC thank the support from the Ministry of Science and Technology, Taiwan, under grant Nos. MOST 110-2112-M-001-068-MY3 and MOST 111-2112-M-001-038-MY3 and the Academia Sinica, Taiwan, under grant Nos. AS-CDA-111-M04 and AS-IA-112-M04. SO and MM acknowledge the financial contribution from the PRIN INAF 2019 grant “From massive stars to supernovae and supernova remnants: driving mass, energy and cosmic rays in our Galaxy”. The DOE NNSA-ASC OASCR Flash Center at the University of Chicago partly developed the software used in this work. The numerical calculations were carried out complementarily on Yukawa-21 (YITP, Kyoto Univ.), Cray XC50 (CfCA, NAOJ), and HOKUSAI (RIKEN).